JOURNAL OF GEOPHYSICAL RESEARCH, VOL. 114, D14104, doi:10.1029/2008JD011637, 2009

Influence of the Southern Oscillation on tropospheric temperature

J. D. McLean,[1] C. R. de Freitas,[2] and R. M. Carter[3]

Received 16 December 2008; revised 23 March 2009; accepted 14 May 2009; published 23 July 2009.

[1] Time series for the Southern Oscillation Index (SOI) and global tropospheric temperature anomalies (GTTA) are compared for the 1958–2008 period. GTTA are represented by data from satellite microwave sensing units (MSU) for the period 1980–2008 and from radiosondes (RATPAC) for 1958–2008. After the removal from the data set of short periods of temperature perturbation that relate to near-equator volcanic eruption, we use derivatives to document the presence of a 5- to 7-month delayed close relationship between SOI and GTTA. Change in SOI accounts for 72% of the variance in GTTA for the 29-year-long MSU record and 68% of the variance in GTTA for the longer 50-year RATPAC record. Because El Niño–Southern Oscillation is known to exercise a particularly strong influence in the tropics, we also compared the SOI with tropical temperature anomalies between 20°S and 20°N. The results showed that SOI accounted for 81% of the variance in tropospheric temperature anomalies in the tropics. Overall the results suggest that the Southern Oscillation exercises a consistently dominant influence on mean global temperature, with a maximum effect in the tropics, except for periods when equatorial volcanism causes ad hoc cooling. That mean global tropospheric temperature has for the last 50 years fallen and risen in close accord with the SOI of 5–7 months earlier shows the potential of natural forcing mechanisms to account for most of the temperature variation.

Citation: McLean, J. D., C. R. de Freitas, and R. M. Carter (2009), Influence of the Southern Oscillation on tropospheric temperature, *J. Geophys. Res.*, *114*, D14104, doi:10.1029/2008JD011637.

1. Introduction

[2] The El Niño–Southern Oscillation (ENSO) is a tropical Pacific atmosphere-ocean phenomenon but its influence on climate can be seen globally [*Allan*, 1988; *Allan et al.*, 1996; *Trenberth and Caron*, 2001; *Trenberth et al.*, 2002; *Fernandez et al.*, 2004]. The detailed mechanisms driving these changes are unclear but large-scale changes in global circulation are involved.

[3] During La Niña events, the zonal circulation of the Walker Circulation is enhanced and becomes pronounced, with well-defined and vigorous rising and sinking branches. This results in stronger than normal easterly equatorial surface winds. In contrast, during El Niño events, there is an increase in meridional Hadley cell circulation and subtropical highs intensify, although the relationship between the enhanced regional Hadley cell and warm-phase ENSO cycle circulation anomalies is not always straightforward [*Bhaskaran and Mullan*, 2003]. A more vigorous overturning of the Hadley Cell circulation leads to an increase in heat transfer from tropical to higher latitudes in both hemispheres [*Oort and Yienger*, 1996] and *Bhaskaran and Mullan* [2003] found that during La Niña conditions the Hadley cell in both hemispheres weakens. The anomalies in the strength of the Hadley Cell Circulation are also strongly and inversely correlated with the anomalies in the strength in the Walker Circulation. As meridional circulation increases during El Niño events, there are teleconnections globally [e.g., *Indeje et al.*, 2000; *Janicot et al.*, 2001; *Ntale and Gan*, 2004; *Giannini et al.*, 2001]. It seems clear, therefore, that the ENSO signal is correlated with climate variation, which in turn is reflected in mean global temperature. The extent to which ENSO is related to the latter may be a key to successful extended climate forecasts [*Mullan*, 1996].

[4] The extent to which ENSO forcing explains variance in the mean global temperature record has been the subject of several studies [*Fernandez et al.*, 2004; *Michaels and Knappenberger*, 2000; *Sobel et al.*, 2002], but the additional record in the satellite tropospheric temperature observations since publication of *Fernandez et al.* [2004] provides the opportunity to investigate this further. In our study we quantify the effect of possible ENSO forcing on mean global temperature, both short-term and long-term, and then examine the implications.

2. Data

[5] We use two instrumental data sets of tropospheric temperature. The first is the University of Alabama in Huntsville (UAH) lower-tropospheric (LT) temperature data (http://vortex.nsstc.uah.edu/public/msu/t2/uahncdc.mt)

[1]Applied Science Consultants, Croydon, Victoria, Australia.
[2]School of Geography, Geology and Environmental Science, University of Auckland, Auckland, New Zealand.
[3]Marine Geophysical Laboratory, James Cook University, Townsville, Queensland, Australia.

0148-0227/09/2008JD011637$09.00

Table 1. Major Volcanic Eruptions, 1961–2008[a]

Location	Duration	VEI	DVIG
Agung	Feb 1963 to Jan 1964	5	800
Awu	Aug 1966 to Oct 1966	4	200
El Chichón	Mar 1982 to Sep 1982	5	800
Pinatubo	Apr 1991 to Sep 1991	6	not given

[a]VEI, volcanic explosivity index; DVIG, global Dust Veil Index values.

based on measurements from selected view angles of Microwave Sounding Unit (MSU) channel LT 2 (see *Christy et al.* [2000] and updates). The second is the balloon-based instrumentation (radiosondes). The MSUs measure upwelling longwave radiation emitted by oxygen molecules and temperature is derived from this radiation [*Spencer and Christy*, 1992]. We use global monthly anomalies for the period December 1979 to June 2008, based on the most recent revision of data which incorporate corrections for the effects of orbital decay and east–west drift of the MSU satellites and for differences between MSU instruments that have been added or removed during the measurement period (see *Wentz and Schabel* [1998] and *Christy et al.* [2000] and updates).

[6] The MSU data are accurate to 0.1°C and monitor the atmospheric temperature of the whole planet in a consistent fashion and free of the local influences at the Earth's surface. This is in contrast with data collected using thermometers at observation stations, which are near or at the Earth's surface, mainly on land, predominantly in the Northern Hemisphere and often located in or near urban areas. However, a drawback of the MSU data is that their collection only commenced in 1979, so to extend this time period we have supplemented the MSU data with measurements made by balloon-mounted radiosondes. NOAA and the U.S. National Climate Data Center provide collated data on tropospheric temperatures from balloon-based instrumentation since 1958, assembled into the Radiosonde Atmospheric Temperature Products for Assessing Climate (RATPAC) product [*National Climatic Data Center*, 2008]. These data are of coarser granularity than MSU data, but *Lanzante et al.* [2003] show that the differences are slight. Here we use the RATPAC-A tropospheric temperature data designated "850 to 300 mb," which represents the atmospheric layer approximately between 1500 m (5000 feet) and 9000 m (30,000 feet). Geographical sparsity and seasonal granularity are drawbacks to the RATPAC-A but nonetheless these are the best tropospheric data available prior to the introduction of satellite-based systems. Data from MSU and RATPAC-A are used to calculate global tropospheric temperature anomalies (GTTA) from period means.

[7] To represent ENSO variability, we use the Southern Oscillation Index (SOI) provided by the Australian Government Bureau of Meteorology ("S.O.I. (Southern Oscillation Index) Archives: 1876 to present, accessed 1 December 2008, available at http://www.bom.gov.au/climate/current/soihtm1.shtml). The SOI is used here is the Troup SOI, which is the standardized anomaly of the seasonal mean sea level pressure difference between Tahiti and Darwin, divided by the standard deviation of the difference and multiplied by 10 [*Troup*, 1965]. Using this method, the SOI ranges from about −35 to about +35 with negative values associated with El Niño conditions and positive values with La Niña.

[8] Data for volcanic eruptions that are relevant to this discussion are shown in Table 1. The Volcanic Explosivity Index (VEI) values are according to the Smithsonian Institute's extension of work by *Newhall and Self* [1982] and indicate the impact on stratospheric aerosol optical depth and hence on climate. A VEI of 4 indicates ejecta volume >0.1 km^3, VEI 5 of >1 km^3 and VIE 6 of >10 km^3. The Dust Veil Index values are according to *Lamb* [1970, 1977, 1983], who regarded values greater than 100 as significant. We use the global Dust Veil Index values (hence DVIG) rather than hemispheric because this discussion relates to global average temperature.

[9] The volcanoes listed in Table 1 are all located near either the western or eastern ends of the Pacific. Those eruptions on the western side of the Pacific may have disrupted circulation patterns of the ENSO system or, via local weather conditions, indirectly influenced the air pressures from which the SOI is calculated, whereas those eruptions on the eastern side of the Pacific may have disrupted the easterly trade winds that are characteristic of neutral or La Niña conditions. That these volcanoes are all in the vicinity of the tropics is important as ENSO is a tropical phenomena, albeit with influence outside that zone. Also, about 50% of the Earth's surface is within 30°N to 30°S, with circulation to both hemispheres driven from there.

3. Analysis and Results

[10] We start by considering 12-month running averages of our data. This approach can minimize significant data and give undue emphasis to insignificant data, so we use it here mainly to establish a contextual record.

[11] Figure 1 shows the 12-month running average of the SOI and GTTA from 1979, with the SOI plot inverted because temperature is the primary concern. The first half of this graph shows poor correlation, but this was a period with a number of volcanic eruptions where the temperatures fall after an eruption and subsequently recover as ejected matter slowly disappears from the atmosphere. The latter half (post-1996) shows a generally more consistent relationship and indicates that a change in SOI has a corresponding but delayed change in GTTA.

[12] To examine the relationship between SOI and GTTA, the data for the period of volcanic eruptions were removed along with the data for the subsequent 12 months; the latter being required in order that the 12-month running averages do not include data from periods of volcanic activity. Care has been taken to determine the last of any series of eruptions but this approach is still not ideal because the climatic influence of volcanoes can be delayed (*Douglass and Knox* [2005] estimated 6.5 months for the Pinatubo eruption of 1991) and can continue for up to 2–3 years or more after the eruption. Taking into account a period of climatic influence beyond the eruption dates (influence of data in the 12-month averages) would require assumptions and estimates of the discharge, of sulphurs and silicates in particular.

[13] The next step was to determine correlation coefficients for various time lags between a change in SOI and a

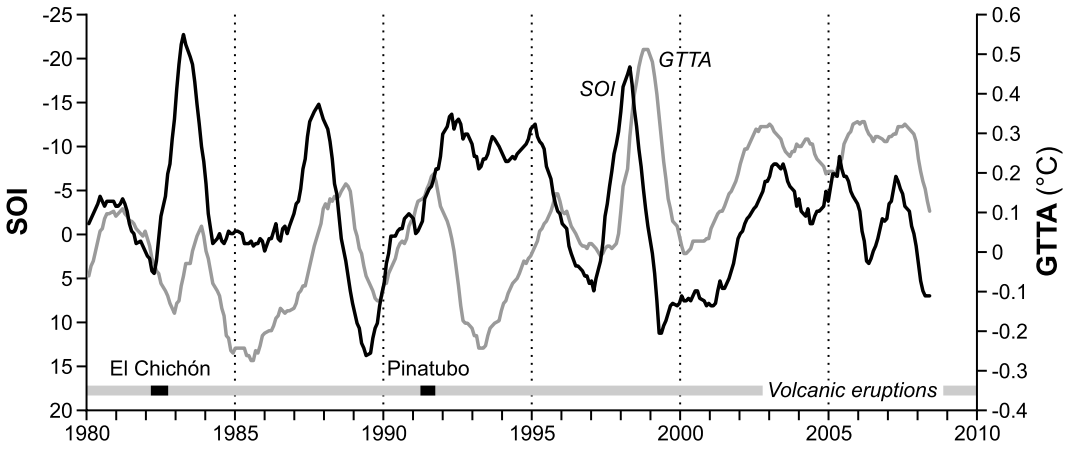

Figure 1. Twelve-month running means of SOI (dark line) and MSU GTTA (light line) for the period 1980 to 2006 with major periods of volcanic activity indicated.

corresponding change in GTTA. A 5-month lag produced the best match of key turning points but the overall correlation of −0.223 is quite weak. This weak correlation may be due to the period during which volcanic eruptions exert an influence on temperature, or to noise caused by short-term forces such as wind, within the two data signals, both of which are given as monthly averages, from which these 12-month running averages were calculated.

[14] To remove the noise, the absolute values were replaced with derivative values based on variations. Here the derivative is the 12-month running average subtracted from the same average for data 12 months later. This technique is essentially the same as comparing successive annual averages but we extend it across all months. For this calculation we must extend the exclusion period for volcanic eruptions by a further 12 months in order to remove it from our calculations. Figure 2 shows the derivatives of SOI and GTTA with optimum fit of a 7-month time lag (Figure 3) between the two factors. This approach produces a correlation coefficient for the derivatives of SOI (dSOI) and GTTA (dGTTA) of −0.847 and the line of best fit is

$$\mathrm{dGTTA} = -0.0149 * \mathrm{dSOI} + 0.0424, \quad (1)$$

with $R^2 = 0.72$ and where dGTTA applies 7 months after dSOI.

[15] To examine a longer time period, the seasonal (i.e., 3-month mean) RATPAC-A data from 1960 to 2007 were used. Figure 4 shows the RATPAC-A data and the corresponding 3-month averages of SOI, with major volcanic eruptions indicated. The two earliest volcanic eruptions shown in Table 1 are now included because the RATPAC data extend back to 1960.

[16] By using our earlier technique of derivatives with exclusions for volcanic eruptions, but with a time lag of 6 months, the line of best fit was determined to be

$$\mathrm{dGTTA} = -0.0189 * \mathrm{dSOI} + 0.0326, \quad (2)$$

where $R^2 = 0.68$.

[17] Figure 5 shows the derivatives of the SOI (time shifted) and RATPAC-A LTT from 1961, with periods of volcanic activity indicated.

[18] If, as the results so far indicate, the Southern Oscillation impacts on the GTTA then an even stronger relationship is to be expected between the SOI and tropospheric temperature anomalies in the tropics [*Kumar et al.*, 2006],

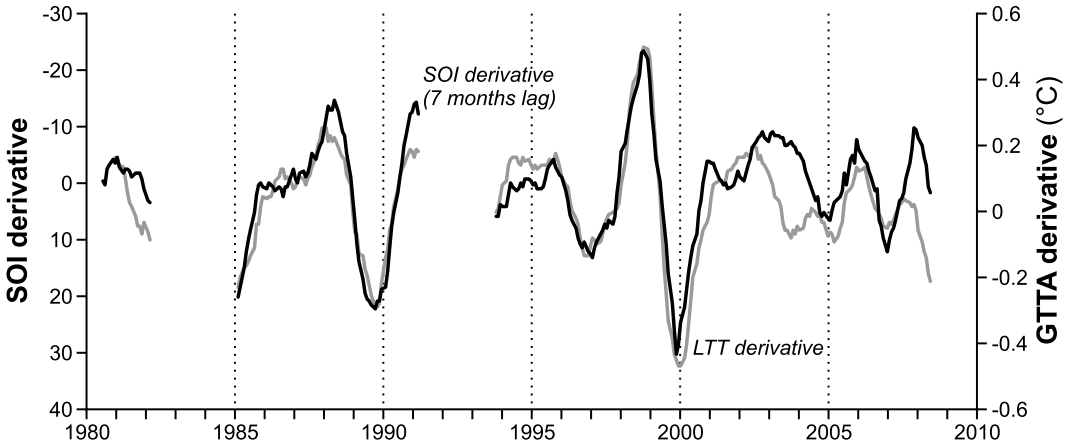

Figure 2. Derivatives of SOI (dark line) and MSU GTTA (light line) for the period 1981–2007 after removing periods of volcanic influence ($R^2 = 0.72$). Start date for data is 1981 because of the calculation of derivatives.

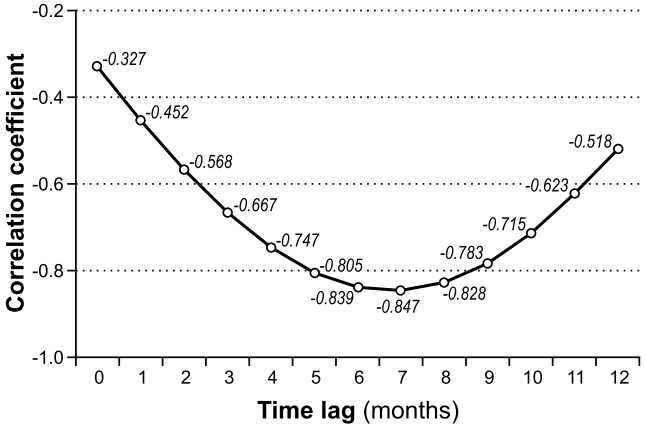

Figure 3. Correlation coefficients for 12-month running means of SOI and GTTA with different time lags.

where this region is defined as the area bounded by latitudes 20°N and 20°S. Figure 6 shows this to be the case.

[19] Using the same technique of derivatives with data exclusions for periods of volcanic activity the line of best fit is

$$\mathrm{dLTT\,(trop)} = -0.0311 * \mathrm{dSOI} + 0.0252, \quad (3)$$

where $R^2 = 0.81$. In this case the optimum time lag is 5 months rather than the 7 months for global temperature data. The difference in ±1 month is slight; with a 4-month delay $R^2 = -0.80$, and with a 6-month delay $R^2 = -0.78$.

4. Discussion

[20] The results reported here show a delayed relationship between the state of the Southern Oscillation and the average global tropospheric temperature. This relationship has held for as long as lower tropospheric temperatures have been monitored and the change from RATPAC-A to MSU-based data makes little difference to its manifestation. The strength of the relationship with global and tropical temperatures is indicative of the increased vigor in the meridional dispersal of heat during El Niño conditions and the delay in the temperature response is consistent with the transfer of tropical heat.

[21] A likely explanation for this relationship is the vigor of the Hadley Cell circulation and its distribution of warm air surface ocean water from the tropical regions to higher latitudes. This circulation is weak when the Southern Oscillation is in a neutral or La Niña state (i.e., near-zero or positive SOI values) but strengthens as the Southern Oscillation moves to a condition consistent with a negative SOI [*Bhaskaran and Mullan*, 2003; *Oort and Yienger*, 1996].

[22] The transfer of tropical heat to the Arctic increases as SOI trends toward El Niño conditions. This transfer of heat, estimated by *Trenberth and Caron* [2001] to be about 5 petawatts at midlatitudes during El Niño events, can account for local warming in the Arctic and the consequent decrease in sea ice extent, although the latter is probably also influenced by water temperature which in turn is driven by the transport of heat by ocean currents that operate on a longer time constant (~1000 years) than does the atmosphere.

[23] The analysis using lower tropospheric temperature (see derivatives) determined an optimum delay of 7 months but may not have excluded all periods influenced by volcanic activity. The RATPAC-A data have a granularity of 3 months and, as with the tropical UAH LTT, the variation in R is very minor for the month either side of the optimum time lag. In our opinion the 7-month delay, determined by the analysis of derivatives of UAH MSU lower tropospheric temperature data, is probably the optimum period. Figure 7 shows the relationship when a 7-month delay is introduced, first using the seasonal RATPAC temperature data (1958–1980) and then between MSU LTT data.

[24] The above results contrast with the results of work by *Yulaeva and Wallace* [1994] who found that mean tropical temperatures for a 13-year record lagged outgoing longwave anomalies by about 3 months; while *Trenberth et al.* [2002] found warming events peak 3 months after sea surface temperature (SST) in the Niño-3.4 region. However, the robustness of this observed lag is not yet clear, since *Kumar and Hoerling* [2003] found lags between 1 and 3 months with SST in the Niño-3.4 region for the period

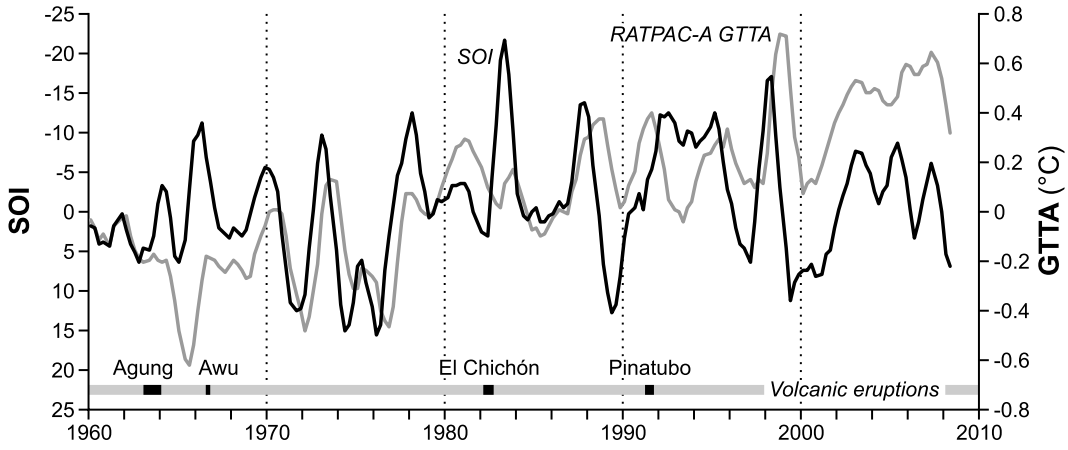

Figure 4. Twelve-month running means of SOI (dark line) and RATPAC-A GTTA (light line) for the period 1960–2008 with principal volcanic activity indicated.

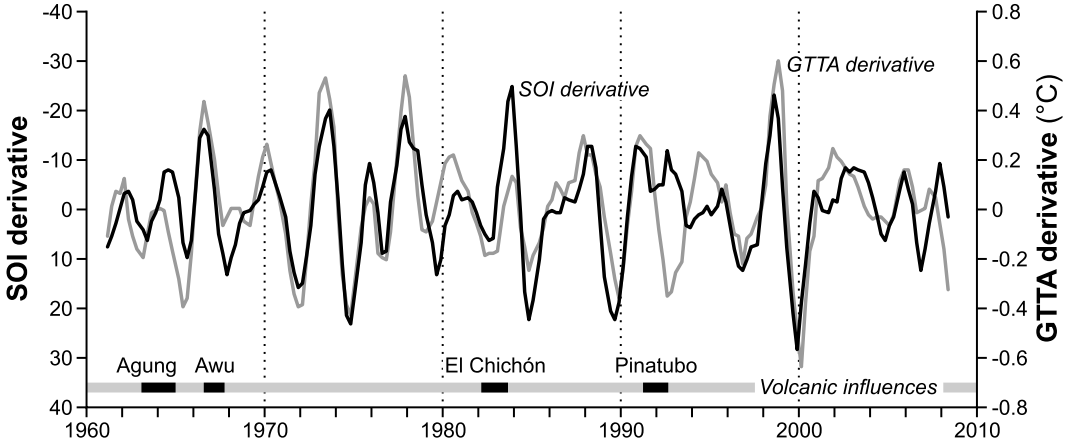

Figure 5. The derivatives of the SOI (dark line) and RATPAC-A GTTA (light line) across the full period for which both sets of data are available (1961–2008). Periods of volcanic activity are also indicated. Start date for data is 1961 because of the calculation of derivatives.

1950–1999. *Sobel et al.* [2002] determined that the correlation between SST in the Niño-3 region and the GGTA was optimum with a time lag of 3–6 months. Here we use the atmospheric component of ENSO, the Southern Oscillation, rather than SST and show an optimum correlation of 7 months.

[25] The dominant disruption to the relationship between the Southern Oscillation and mean global temperature appears to be related to volcanic activity in the equatorial belt, particularly in the Pacific Ocean. Volcanic eruptions affect climate by injecting sulphur dioxide into the stratosphere where it is converted into sulphate aerosols that reflect incoming solar radiation [*Lacis et al.*, 1992; *Sato et al.*, 1993]. This reduces the amount of solar energy absorbed at the Earth's surface and ultimately the energy available for heating the troposphere [*Mass and Portman*, 1989; *Dutton and Christy*, 1992].

[26] Figure 7a shows the volcanic activity noted earlier, including Awu (August–October 1966, VEI = 4, DVIG = 200). Volcanic activity may well be the cause of other small breakdowns in the relationship but which of numerous possible volcanoes are responsible is not clear. Eruptions at the western side of the Pacific, of Colo (July 1983 to December 1983, VEI = 4, DVIG = unknown) and Rabaul (September 1994 to April 1995, VEI = 4, DVIG = unknown), may have negatively influenced the Hadley Cell Circulation that accompanies El Niño events, and eruptions at the eastern side of the Pacific (e.g., Hawaii's Mauna Loa and Colombia's Nevado del Ruiz) may have suppressed easterly winds across the Pacific and either induced an El Niño or influenced the atmospheric conditions from which the SOI is calculated. *Wigley* [2000] proposed that El Niño events occur shortly after volcanic eruptions and *Emile-Geay et al.* [2008] claimed that volcanic eruptions increased the probability of El Niño events. However, there is insufficient information available at present to support such speculation.

[27] The frequent volcanic eruptions prior to 1995 often depressed the GTTA and no volcano-free period prior to 1995 is of sufficient length to properly compare trends in GTTA and SOI. The post-1995 period illustrated in Figure 7c shows that the respective trends across the last 14 years

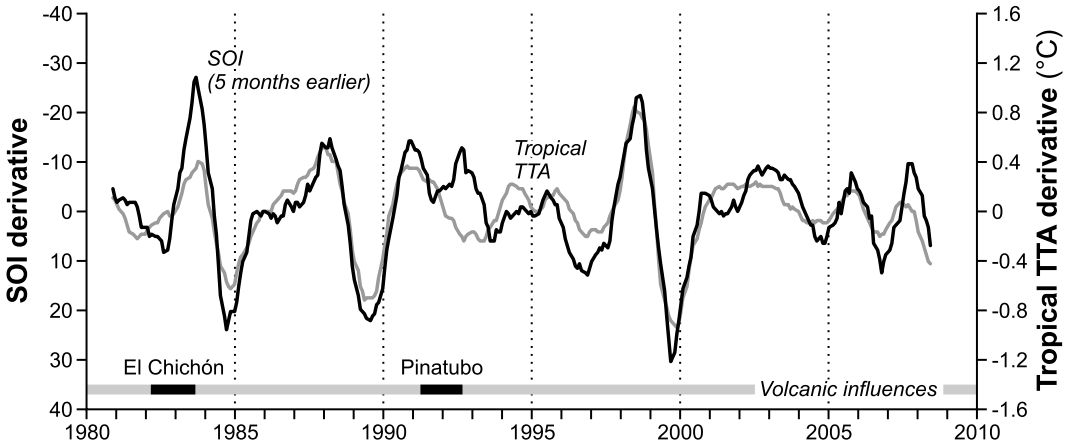

Figure 6. Derivatives of SOI (dark line) and UAH tropospheric temperature anomalies (light line) in the tropics, with SOI from 5 months earlier. The indicated periods of volcanic activity were excluded from calculations. Start date for data is 1981 because of the method of calculation of derivatives.

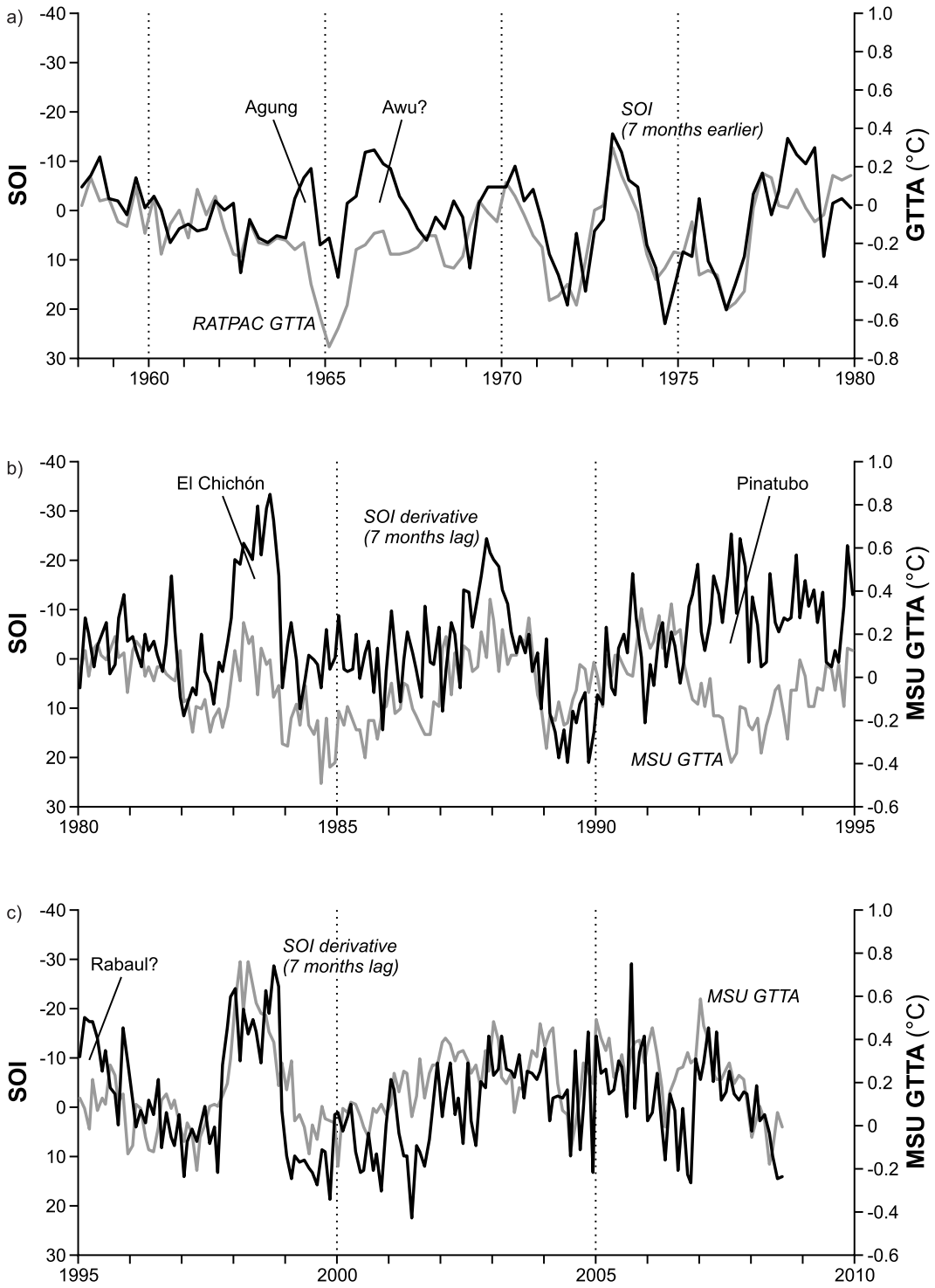

Figure 7. Seven-month shifted SOI with (a) seasonal RATPAC-A GTTA data 1958–1979 and monthly UAH MSU GTTA data (b) 1980–1995 and (c) 1995–2008. Dark line indicates SOI, and light line indicates lower tropospheric temperature. Periods of volcanic activity are indicated (see text). Question marks alongside certain volcanic eruptions refer to the uncertainty of their impact.

will be very similar, albeit from 1997 onward the average global temperature anomaly is consistently slightly higher than the relationship would suggest (see Figure 7c). This situation is consistent with a recorded variation in cloud cover. According to data from the International Satellite Cloud Climatology Project (ISCCP), from 1984 to 2005 midlevel cloud cover in the tropics was relatively constant but both lower- and upper-level cloud cover declined slightly. In the exotropics (latitude >20°) of both hemispheres upper level cloud remained relatively constant at around 12% of sky cover, but from 1998 low-level cloud progressively decreased while midlevel and upper-level

cloud increased. The reasons for this change are not clear, nor is it clear whether the change is a cause or effect of the parallel temperature change [*Spencer and Braswell*, 2008].

[28] The relationship between the delayed SOI and lower tropospheric temperature is generally good on a large scale but less so for individual months. This is consistent with the operation of short-term weather forces (e.g., wind, pressure cell dynamics) acting on both factors.

[29] The Great Pacific Climate Shift of 1976 [*Guilderson and Schrag*, 1998] appears to have had an effect on the SOI and therefore on the GTTA. The abruptness of this change suggests a major physical event, but no definite cause has been established. *McPhaden and Zhang* [2002] report a significant decrease in the estimated cold-water upwelling since that time. This implies a warmer Pacific Ocean and a bias toward El Niño events, but it is unclear whether this is a cause or consequence of the shift. Figure 4 shows that the change in SOI, in February or March of 1976, was followed by a corresponding change in GTTA in the last few months of the year. The granularity of the RATPAC-A GTTA data prevents clear identification of the time of change but it appears to be consistent with the time lag reported here.

[30] For the 30 years prior to the 1976 shift (i.e., 1946–1975) the SOI averaged +1.93 but in the 30 years after 1976 (i.e., 1977–2006) the average was −3.06, which represents a shift from a La Niña inclination to an El Niño inclination. The standard deviations for the two periods were 9.48 and 10.40 on monthly SOI averages, and 6.56 and 6.35 on calendar year averages, which indicates consistent variation about a new average value. Only the RATPAC-A data are available for lower tropospheric temperatures both before and after this shift, and even then we are limited to 17-year periods for our analysis of RATPAC-A data because monitoring did not commence until mid-1958. From 1959 to 1975 the RATPAC LTT averaged −0.191°C and from 1977 to 1993 it averaged +0.122°C. The standard deviations on the seasonal data were 0.193° and 0.163 C°, and on monthly data 0.162°C and 0.146°C. We have already illustrated the close relationship between SOI and GTTA, but this description of the respective changes before and after the Great Pacific Climate Shift indicates a stepwise shift in the base values of each factor but otherwise relatively consistent ranges of variation.

[31] The findings presented here are consistent with the Southern Oscillation being a major driver of temperature anomalies, not only in the tropics but also on a global scale. In passing we also note that according to the relationship between SOI and GTTA, 1983–1984 would likely have been about as warm as 1998 if not for the cooling influence of El Chichón.

[32] *Lean and Rind* [2008] stated that anthropogenic warming is more pronounced between 45°S and 50°N and that no natural process can account for the overall warming trend in global surface temperature. We have shown here that ENSO and the 1976 Great Pacific Climate Shift can account for a large part of the overall warming and the temperature variation in tropical regions. We also note that Figure 1 of *Lean and Rind* [2008], based on a different temperature data set to that used here, indicates that their model underestimated temperatures during and immediately following the predominantly El Niño conditions from September 1939 to January 1942, and overestimated temperatures during and immediately following the La Niña dominated period from August 1906 to December 1910. This suggests that their model poorly replicated ENSO effects.

[33] Chapter 3 of the Working Group I contribution to the Fourth Assessment Report by the *Intergovernmental Panel on Climate Change* (*IPCC*) [2007] notes the strong relationship between the ENSO and various climate phenomena, including surface temperature. Chapter 8 reports "considerable model skill out to 12 months for ENSO prediction." Chapter 9 raises the question of ENSO response to continued anthropogenic warming, although causal connections are not clear. However, nowhere does *IPCC* [2007] mention the delay between a change in ENSO and a corresponding change in GTTA, which we have shown here to be 7 months. Climate modelers acknowledge that their models do not adequately hindcast average global temperatures from 1950 to 1990 and apply a human influence factor to make up the deficit. The strength of the time lagged relationship between ENSO and GTTA, as demonstrated here, suggests that variation in the poorly modeled ENSO may account for the deficit and may be the cause of a large part of the observed warming since the midtwentieth century. The sequence of the lagged relationship indicates that ENSO is driving temperature rather than the reverse. Reliable ENSO prediction is possible only to about 12 months [*IPCC*, 2007], which implies that accurate temperature forecasting beyond that period will only be possible after improvements in ENSO prediction.

5. Conclusion

[34] We have shown that the Southern Oscillation is a dominant and consistent influence on mean global temperature. Shifts in temperature are consistent with shifts in the SOI that occur about 7 months earlier. The relationship weakens or breaks down at times of volcanic eruption in the tropics, and meridional heat dispersal likely accounts for this.

[35] The slight fall in temperatures prior to the Great Pacific Climate Shift can be attributed to the increasing dominance of positive SOI values (i.e., toward La Niña) leading up to that event and the rise in temperatures following the shift can be attributed to the dominance of negative SOI values since (i.e., a period of extended El Niño tendencies).

[36] Since the mid-1990s, little volcanic activity has been observed in the tropics and global average temperatures have risen and fallen in close accord with the SOI of 7 months earlier. Finally, this study has shown that natural climate forcing associated with ENSO is a major contributor to variability and perhaps recent trends in global temperature, a relationship that is not included in current global climate models.

[37] **Acknowledgment.** We thank Craig Loehle for comments on aspects of the statistical analysis used in the study.

References

Allan, R. J. (1988), El Niño Southern Oscillation influences in the Australasian region, *Prog. Phys. Geogr.*, *12*, 313–348, doi:10.1177/030913338801200301.

Allan, R. J., J. Lindesay, and D. Parker (1996), *El Niño Southern Oscillation and Climatic Variability*, CSIRO Publ., Collingwood, Victoria, Australia.

Bhaskaran, B., and A. B. Mullan (2003), El Niño-related variations in the southern Pacific atmospheric circulation: Model versus observations, *Clim. Dyn.*, *20*, 229–239.

Christy, J. R., R. W. Spencer, and W. D. Braswell (2000), MSU tropospheric temperatures: Dataset construction and radiosonde comparison, *J. Atmos. Oceanic Technol.*, *17*, 1153–1170, doi:10.1175/1520-0426(2000)017<1153:MTTDCA>2.0.CO;2.

Douglass, D., and R. S. Knox (2005), Climate forcing by the volcanic eruption of Mount Pinatubo, *Geophys. Res. Lett.*, *32*, L05710, doi:10.1029/2004GL022119.

Dutton, E. G., and J. R. Christy (1992), Solar radiative forcing at selected locations and evidence for global lower tropospheric cooling following the eruptions of El Chichón and Pinatubo, *Geophys. Res. Lett.*, *19*(23), 2313–2316, doi:10.1029/92GL02495.

Emile-Geay, J., R. Seager, M. A. Cane, E. R. Cook, and G. H. Haug (2008), Volcanoes and ENSO over the past millennium, *J. Clim.*, *21*, 3134–3148, doi:10.1175/2007JCLI1884.1.

Fernandez, N. C., R. G. Herrera, D. G. Puyol, E. H. Martin, R. R. Garcia, L. G. Presa, and P. R. Rodriguez (2004), Analysis of the ENSO signal in tropospheric and stratospheric temperatures observed by MSU, 1979–2000, *J. Clim.*, *17*, 3934–3946, doi:10.1175/1520-0442(2004)017<3934:AOTESI>2.0.CO;2.

Giannini, A., J. C. H. Chiang, M. A. Cane, Y. Kushnir, and R. Seager (2001), The ENSO teleconnection to the tropical Atlantic Ocean: Contributions of the remote and local SSTs to rainfall variability in the tropical Americas, *J. Clim.*, *14*, 4530–4544, doi:10.1175/1520-0442(2001)014<4530:TETTTT>2.0.CO;2.

Guilderson, T. P., and D. P. Schrag (1998), Abrupt shift in subsurface temperatures in the tropical Pacific associated with changes in El Niño, *Science*, *281*, 240–243, doi:10.1126/science.281.5374.240.

Indeje, M., H. M. Semazzi, and L. J. Ogallo (2000), ENSO signals in East African rainfall seasons, *Int. J. Climatol.*, *20*, 19–46, doi:10.1002/(SICI)1097-0088(200001)20:1<19::AID-JOC449>3.0.CO;2-0.

Intergovernmental Panel on Climate Change (IPCC) (2007), *Climate Change 2007: The Physical Science Basis. Contribution of Working Group I to the Fourth Assessment Report of the Intergovernmental Panel on Climate Change*, edited by S. Solomon et al., Cambridge Univ. Press, Cambridge, U. K.

Janicot, S., S. Trzaska, and I. Poccard (2001), Summer Sahel-ENSO teleconnections and decadal time scale SST Variations, *Clim. Dyn.*, *18*, 303–320, doi:10.1007/s003820100172.

Kumar, A., and M. P. Hoerling (2003), The nature and causes for the delayed atmospheric response to El Niño, *J. Clim.*, *16*, 1391–1403.

Kumar, K. K., B. Rajagopalan, M. Hoerling, G. Bates, and M. Cane (2006), Unraveling the mystery of Indian monsoon failure during El Niño, *Science*, *314*, 115–119, doi:10.1126/science.1131152.

Lacis, A., J. Hansen, and M. Sato (1992), Climate forcing by stratospheric aerosols, *Geophys. Res. Lett.*, *19*(15), 1607–1610, doi:10.1029/92GL01620.

Lamb, H. H. (1970), Volcanic dust in the atmosphere: With a chronology and assessment of its meteorological significance, *Philos. Trans. R. Soc. A*, *266*, 425–533, doi:10.1098/rsta.1970.0010.

Lamb, H. H. (1977), Supplementary volcanic dust veil assessments, *Clim. Monit.*, *6*, 57–67.

Lamb, H. H. (1983), Update of the chronology of assessment of the volcanic dust veil index, *Clim. Monit.*, *12*, 79–90.

Lanzante, J. R., S. A. Klein, and D. J. Seidel (2003), Temporal homogenization of monthly radiosonde temperature data Part II: Trends, sensitivities and MSU comparison, *J. Clim.*, *16*, 241–262.

Lean, J. L., and D. H. Rind (2008), How natural and anthropogenic influences alter global and regional surface temperature: 1889 to 2006, *Geophys. Res. Lett.*, *35*, L18701, doi:10.1029/2008GL034864.

Mass, C. F., and D. A. Portman (1989), Major volcanic eruptions and climate: A critical evaluation, *J. Clim.*, *2*, 566–593, doi:10.1175/1520-0442(1989)002<0566:MVEACA>2.0.CO;2.

McPhaden, M. J., and D. Zhang (2002), Slowdown of the meridional overturning circulation in the upper Pacific Ocean, *Nature*, *415*, 603–608, doi:10.1038/415603a.

Michaels, P. J., and P. C. Knappenberger (2000), Natural signals in the MSU lower tropospheric temperature record, *Geophys. Res. Lett.*, *27*(18), 2905–2908, doi:10.1029/2000GL011833.

Mullan, A. B. (1996), Effects of ENSO on New Zealand and the South Pacific, in *Prospects and Needs for Climate Forecasting*, edited by D. Braddock, pp. 23–27, R. Soc. of New Zealand, Wellington.

National Climatic Data Center (2008), Radiosonde Atmospheric Temperature Products for Assessing Climate (RATPAC) data, accessed 29 October 2008, http://www.ncdc.noaa.gov/oa/climate/ratpac/index.php?name=access, Asheville, N. C.

Newhall, C. G., and S. Self (1982), The volcanic explosivity index (VEI): An estimate of explosive magnitude for historical volcanism, *J. Geophys. Res.*, *87*(C2), 1231–1238, doi:10.1029/JC087iC02p01231.

Ntale, H. K., and T. Y. Gan (2004), East African rainfall anomaly patterns in association with El Niño/Southern Oscillation, *J. Hydrol. Eng.*, *9*(4), 257–268, doi:10.1061/(ASCE)1084-0699(2004)9:4(257).

Oort, A. H., and J. J. Yienger (1996), Observed interannual variability in the Hadley Circulation and its connection to ENSO, *J. Clim.*, *9*, 2751–2767, doi:10.1175/1520-0442(1996)009<2751:OIVITH>2.0.CO;2.

Sato, M., J. E. Hansen, M. P. McCormick, and J. B. Pollack (1993), Stratospheric Aerosol Optical Depths, 1850–1990, *J. Geophys. Res.*, *98*(D12), 22,987–22,994, doi:10.1029/93JD02553.

Sobel, A. H., I. M. Held, and C. S. Bretherton (2002), The ENSO signal in tropical tropospheric temperature, *J. Clim.*, *15*, 2702–2706, doi:10.1175/1520-0442(2002)015<2702:TESITT>2.0.CO;2.

Spencer, R. W., and W. D. Braswell (2008), Potential biases in feedback diagnosis from observational data: A simple model demonstration, *J. Clim.*, *21*, 5624–5628, doi:10.1175/2008JCLI2253.1.

Spencer, R. W., and J. R. Christy (1992), Precision and radiosonde validation of satellite gridpoint temperature anomalies. Part II: A tropospheric retrieval and trends during 1979–90, *J. Clim.*, *5*, 858–866, doi:10.1175/1520-0442(1992)005<0858:PARVOS>2.0.CO;2.

Trenberth, K. E., and J. M. Caron (2001), Estimates of meridional atmosphere and ocean heat transports, *J. Clim.*, *14*, 3433–3443, doi:10.1175/1520-0442(2001)014<3433:EOMAAO>2.0.CO;2.

Trenberth, K. E., J. M. Caron, D. P. Stepaniak, and S. Worley (2002), Evolution of El Niño–Southern Oscillation and global atmospheric surface temperatures, *J. Geophys. Res.*, *107*(D8), 4065, doi:10.1029/2000JD000298.

Troup, A. J. (1965), The 'Southern Oscillation,' *Q. J. R. Meteorol. Soc.*, *91*, 490–506, doi:10.1002/qj.49709139009.

Wentz, F. J., and M. Schabel (1998), Effects of satellite orbital decay on MSU lower tropospheric temperature trends, *Nature*, *394*, 661–664, doi:10.1038/29267.

Wigley, T. M. L. (2000), ENSO, volcanoes and record-breaking temperatures, *Geophys. Res. Lett.*, *27*(24), 4101–4104, doi:10.1029/2000GL012159.

Yulaeva, E., and J. M. Wallace (1994), The Signature of ENSO in global temperature and precipitation fields derived from the microwave sounding unit, *J. Clim.*, *7*(11), 1719–1736, doi:10.1175/1520-0442(1994)007<1719:TSOEIG>2.0.CO;2.

R. M. Carter, Marine Geophysical Laboratory, James Cook University, Townsville, Qld 4811, Australia.

C. R. de Freitas, School of Geography, Geology and Environmental Science, University of Auckland, Private Bag 92019, 10 Symonds Street, Auckland 1142, New Zealand. (c.defreitas@auckland.ac.nz)

J. D. McLean, Applied Science Consultants, P.O. Box 314, Croydon, Vic 3136, Australia.